

# First-Principles Calculation of $^{17}\text{O}$ and $^{25}\text{Mg}$ NMR Shieldings in MgO at Finite Temperature: Rovibrational Effect in Solids

**Stéphanie Rossano\***

*Laboratoire des Géomatériaux, Université de Marne la Vallée, CNRS FRE2455, 5 Bd Descartes, Champs/Marne, 77454 Noisy-Champs Cedex 2, France*

**Francesco Mauri**

*Laboratoire de Minéralogie-Cristallographie, Université Pierre et Marie Curie, 4 place Jussieu, Case Postale 115, 75252 Paris Cedex 05, France*

**Chris J. Pickard**

*TCM Group, Cavendish Laboratory, Madingley Road, Cambridge CB3 0HE, United Kingdom*

**Ian Farnan**

*Department of Earth Sciences, University of Cambridge, Downing Street, Cambridge CB2 3EQ, United Kingdom*

*Received: December 17, 2004; In Final Form: February 17, 2005*

The temperature dependence of  $^{17}\text{O}$  and  $^{25}\text{Mg}$  NMR chemical shifts in solid MgO have been calculated using a first-principles approach. Density functional theory, pseudopotentials, a plane-wave basis set, and periodic boundary conditions were used both to describe the motion of the nuclei and to compute the NMR chemical shifts. The chemical shifts were obtained using the gauge-including projector augmented wave method. In a crystalline solid, the temperature dependence is due to both (i) the variation of the averaged equilibrium structure and (ii) the fluctuation of the atoms around this structure. In MgO, the equilibrium structure at each temperature is uniquely defined by the cubic lattice parameters, which we take from experiment. We evaluate the effect of the fluctuations within a quasiharmonic approximation. In particular, the dynamical matrix, defining the harmonic Hamiltonian, has been computed for each equilibrium volume. This harmonic Hamiltonian was used to generate nuclear configurations that obey quantum statistical mechanics. The chemical shifts were averaged over these nuclear configurations. The results reproduce the previously published experimental NMR data measured on MgO between room temperature and 1000 °C. It is shown that the chemical shift behavior with temperature cannot be explained by thermal expansion alone. Vibrational corrections due to the fluctuations of atoms around their equilibrium position are crucial to reproduce the experimental results.

## 1. Introduction

High-temperature nuclear magnetic resonance (NMR) spectroscopy is a powerful tool for probing the structural and dynamical properties of materials (see ref 1 for a review). However, the interpretation of chemical shift variation with temperature as being due to structural changes should be made with care since thermally induced changes in chemical shifts can also be due to bond expansion or changes in the electronic character of the bond. The presence of low-lying excited states<sup>2</sup> that become populated as temperature increases or an increased time-averaged bond overlap<sup>3</sup> at high temperature have both been proposed as mechanisms for “pure” temperature effects.

To experimentally evaluate the influence of the thermal effects on NMR signals, Fiske and co-workers<sup>4</sup> have measured  $^{25}\text{Mg}$  and  $^{17}\text{O}$  chemical shift variations with temperature in periclase, MgO. Periclase is indeed an ideal compound to probe the “pure”

effect of temperature because it displays a cubic NaCl structure and shows no phase transition up to the melting point (2852 °C).

In the study of Fiske and co-workers,<sup>4</sup> the  $^{25}\text{Mg}$  chemical shift in MgO increases linearly from 25 ppm at room temperature to 27 ppm at 1300 °C, while the  $^{17}\text{O}$  chemical shift in MgO increases linearly from 47 to 57 ppm over the same temperature range. This decrease in shielding of  $^{17}\text{O}$  and  $^{25}\text{Mg}$  in MgO with increasing temperature is not what would be predicted from simple empirical relationships between chemical shift and Mg–O bond distance; previous studies have indeed shown that an increase in the cation–oxygen bond distance either due to an increase in coordination number<sup>5</sup> or due to a cation change<sup>6</sup> should lead to an increasing cation shielding<sup>5,6</sup> and a deshielding of  $^{17}\text{O}$ .<sup>5</sup>

Through the use of the empirical results described in those studies, the thermal expansion of the MgO bond should cause the chemical shift of  $^{25}\text{Mg}$  to drop from 25 ppm at room temperature to 20 ppm at 1300 °C and not to increase as is

\* Author to whom correspondence should be addressed. E-mail: stephanie.rossano@univ-mlv.fr.

observed experimentally. Concerning the  $^{17}\text{O}$  chemical shift, the observed deshielding by 10 ppm is roughly half that expected based on these empirical trends. Consequently, the behavior of  $^{17}\text{O}$  and  $^{25}\text{Mg}$  chemical shifts in MgO with temperature do not follow a simple bond expansion. However, as shown recently,<sup>7</sup> the main impact of a cation change on the chemical shift is not due to a variation of the oxygen–cation distance but to the interaction between the empty d-orbitals of the cation and the 2p-orbitals of the oxygen. Therefore, a direct evaluation of the impact of the Mg–O distance on the  $^{17}\text{O}$  and  $^{25}\text{Mg}$  chemical shift is required to understand the experimental behavior of the chemical shift as a function of temperature.

The first-principles evaluation of the  $^{17}\text{O}$  chemical shifts in MgO using a cluster model has been performed by Tossell<sup>8</sup> to interpret the variation of chemical shift with temperature. Calculations were performed on a  $\text{OMg}_6(\text{OH})_{12}^{-2}$  cluster using the gauge-including atomic-orbital version of coupled Hartree–Fock perturbation theory as implemented in the program Gaussian 94. However, the calculation failed to reproduce the experimental trend for oxygen. Besides, no information was available on the  $^{25}\text{Mg}$  chemical shift as the cluster model did not have the correct MgO environment for Mg.

To investigate the changes in the electronic character of the MgO bond that could be responsible for these variations, we performed a first-principles calculation of both  $^{17}\text{O}$  and  $^{25}\text{Mg}$  chemical shifts in MgO using a plane-wave code. To avoid surface effects and to ensure a good determination of the electronic structure, periodic boundary conditions are employed so that the system treated consists of a periodically repeated cell. The electronic structure is described in the framework of density functional theory (DFT) using either the local density approximation (LDA) or the generalized gradient approximation (GGA) for the exchange–correlation interaction. Chemical shift calculations are performed using the gauge-including projector augmented wave (GIPAW) method.<sup>9</sup> Because rovibrational effects have been shown to contribute in a nonnegligible way to chemical shielding,<sup>10</sup> vibrations of magnesium and oxygen atoms in the MgO structure have been taken into account.

## 2. Temperature Dependence of Chemical Shifts

The two main effects of temperature on a crystalline structure are (i) the variation of the equilibrium structural parameters (lattice parameters and internal coordinates) and (ii) the fluctuations of the positions of atoms around their equilibrium positions. In the case of MgO, the unit cell is cubic, and atomic positions are fixed by symmetry. Thus, the only free parameter defining the equilibrium structure is the lattice parameter  $a$ . The impact of i on chemical shift values can be evaluated by calculating chemical shifts of  $^{17}\text{O}$  and  $^{25}\text{Mg}$  in cells whose volumes follow MgO thermal expansion law. The influence of ii is more difficult to evaluate. Due to fluctuations, the system is no longer invariant on translation. Thus, we have to consider a supercell containing  $n$  unit cells. The average chemical shift of the  $i$  atom located at the  $\vec{R}_i$  position,  $\langle\delta_i\rangle$ , can be expressed as

$$\langle\delta_i\rangle = \int d\vec{R}_1 d\vec{R}_2 \dots d\vec{R}_N \delta_i(a, \vec{R}_1, \vec{R}_2, \dots, \vec{R}_N) P(a, \vec{R}_1, \vec{R}_2, \dots, \vec{R}_N) \quad (1)$$

where  $N$  is the total number of atoms in the supercell and  $\vec{R}_j$  is the position of the atom  $j$  in the supercell.  $P(a, \vec{R}_1, \vec{R}_2, \dots, \vec{R}_N)$  is the probability of finding the atom  $i$  located at the  $\vec{R}_i$  position.  $\delta_i(a, \vec{R}_1, \vec{R}_2, \dots, \vec{R}_N)$  is the chemical shift of atom  $i$  for a cell parameter  $a$  and for an instantaneous atomic configuration given by the  $\{\vec{R}_j\}$  set of positions. Within the quantum statistical

mechanics framework,  $P(a, \vec{R}_1, \vec{R}_2, \dots, \vec{R}_N)$  is given by

$$P(a, \vec{R}_1, \vec{R}_2, \dots, \vec{R}_N) = \frac{\langle \vec{R}_1, \vec{R}_2, \dots, \vec{R}_N | e^{-H/k_B T} | \vec{R}_1, \vec{R}_2, \dots, \vec{R}_N \rangle}{\int d\vec{R}_1' d\vec{R}_2' \dots d\vec{R}_N' \langle \vec{R}_1', \vec{R}_2', \dots, \vec{R}_N' | e^{-H/k_B T} | \vec{R}_1', \vec{R}_2', \dots, \vec{R}_N' \rangle} \quad (2)$$

where  $H$  is the nuclear Hamiltonian of the system with a lattice parameter  $a$ ,  $T$  the temperature, and  $k_B$  the Boltzmann constant. The exact derivation of an explicit quantum probability law  $P(a, \vec{R}_1, \vec{R}_2, \dots, \vec{R}_N)$  for a real crystal is not possible. The numerical evaluation of  $\langle\delta_i\rangle$  in the quantum framework could be performed by using path integral Monte Carlo techniques<sup>11</sup> based on the Feynman path integral approach.<sup>12</sup> When the temperature is much higher than the Debye temperature ( $T_{\text{Debye}}$ ), the quantum approach tends to the classical one. In this case, classical molecular dynamics or Monte Carlo techniques can then be used to evaluate the average chemical shift.

In the present work, we are interested in obtaining the  $^{17}\text{O}$  and  $^{25}\text{Mg}$  chemical shifts in the 25–1000 °C temperature range. These temperatures are lower or equivalent to the Debye temperature of MgO (between 760 and 950 K according to various studies<sup>13–17</sup>). Therefore, the quantum framework has to be used and molecular dynamics is not appropriate. However, the temperature range investigated is much smaller than the melting temperature of MgO (2852 °C). One can therefore suppose that the effect, on the chemical shifts, of the fluctuations of the atoms around their equilibrium position at a given temperature  $T$  can be described by developing the Hamiltonian of the system at the harmonic level in eq 1. This hypothesis is the base of the quasi-harmonic approximation (QHA) that has been successfully applied to MgO up to a temperature of 1000 K.<sup>18</sup> Within the QHA, the Hamiltonian is given by

$$H_{\text{QH}} = \sum_i \frac{\mathbf{p}_i^2}{2m_i} + U_{\text{eq}} + \frac{1}{2} \sum_{i,j} \vec{u}_i \cdot \mathbf{D}_{ij} \cdot \vec{u}_j \quad (3)$$

Here,  $\mathbf{p}_i$  and  $m_i$  are, respectively, the momentum and the mass of atom  $i$ .  $\vec{u}_i$  is the atomic displacement of atom  $i$  from its equilibrium position.  $U_{\text{eq}}$  is the potential value at crystal equilibrium, and  $\mathbf{D}$  is the dynamical matrix<sup>19</sup> computed at the temperature-dependent lattice parameter  $a$ . This Hamiltonian can be rewritten in terms of the creation and annihilation operators of a normal mode  $K$

$$H = \sum_{K=1}^{3N} H_K \quad (4)$$

$$= \sum_{K=1}^{3N} \hbar \omega_K \left( a_K^\dagger a_K + \frac{1}{2} \right) \quad (5)$$

where  $a_K = (\sqrt{2\hbar\omega_K})^{-1}(p_K + i\omega_K q_K)$ . The normal coordinates  $q_K$  are defined by

$$u_{i\alpha} = \sum_{K=1}^{3N} \frac{q^K}{\sqrt{m_i}} \epsilon_{i\alpha}^K \quad (6)$$

and  $p_K = \dot{q}_K = 1/i\hbar [q_K, H]$ .  $\epsilon^K$  and  $\omega_K$  are the eigenvectors and eigenvalues of the  $\mathbf{C}$  matrix whose elements are defined by  $C_{i\alpha j\beta} = D_{i\alpha j\beta} / \sqrt{m_i m_j}$ .

**TABLE 1: Temperatures, Equilibrium Volumes,  $N_c$  Values, and  $\langle u_i^2 \rangle_{\text{th}}$  and  $\langle u_i^2 \rangle_{\text{conf}}$  Values for Oxygen and Magnesium Atoms**

$T$ (°C)	$\text{vol}^a$ (Å <sup>3</sup> )	$N_c^b$	$\langle u_{\text{Mg}}^2 \rangle_{\text{th}}^c$ (Å <sup>2</sup> )	$\langle u_{\text{Mg}}^2 \rangle_{\text{conf}}^d$ (Å <sup>2</sup> )	$\langle u_{\text{O}}^2 \rangle_{\text{th}}^{e,g}$ (Å <sup>2</sup> )	$\langle u_{\text{O}}^2 \rangle_{\text{conf}}^{f,g}$ (Å <sup>2</sup> )
25	597.2667	4	0.0094	0.0074(8)	0.0103	0.011(1)
350	604.2084	8	0.0182	0.018(2)	0.0183	0.019(2)
691	611.5493	8	0.0286	0.031(3)	0.0283	0.029(3)
1000	618.2525	8	0.0385	0.042(4)	0.0380	0.037(4)

<sup>a</sup>Volume of the MgO supercell following the MgO thermal expansion law derived by Hazen.<sup>21</sup> <sup>b</sup>Number of configurations ( $N_c$ ) considered in the “dynamic calculation” for each temperature. <sup>c</sup> $\langle u_{\text{Mg}}^2 \rangle_{\text{th}}$  theoretical value of mean-square displacement of the Mg atom. <sup>d</sup> $\langle u_{\text{O}}^2 \rangle_{\text{th}}$  theoretical value of mean-square displacement of the O atom. <sup>e</sup> $\langle u_{\text{Mg}}^2 \rangle_{\text{conf}}$  average value of mean-square displacement of the Mg atom over the atoms of the different configurations for each temperature. <sup>f</sup> $\langle u_{\text{O}}^2 \rangle_{\text{conf}}$  average value of mean-square displacement of the O atom over the atoms of the different configurations for each temperature. <sup>g</sup>The confidence interval on  $\langle u_{\text{Mg}}^2 \rangle_{\text{conf}}$  and  $\langle u_{\text{O}}^2 \rangle_{\text{conf}}$  was chosen as  $\pm 1.9799\sigma$  where  $\sigma$  is the statistical standard deviation.

Equation 1 can be simplified using the normal coordinate system of the Hamiltonian matrix. In the normal coordinate basis

$$\langle \delta_i \rangle = \int dq_1 dq_2 \dots dq_{3N} \delta_i(q_1, q_2, \dots, q_{3N}) P(a, q_1, q_2, \dots, q_{3N}) \quad (7)$$

and

$$P(a, q_1, q_2, \dots, q_{3N}) = \prod_{K=1}^{3N} p(q_K) \quad (8)$$

$$= \prod_{K=1}^{3N} \langle q_K | e^{-H_K/k_B T} | q_K \rangle \int dq_K' \times \langle q_K' | e^{-H_K/k_B T} | q_K \rangle \quad (9)$$

$p(q_K)$  is exactly described by a Gaussian distribution, whose width  $x$  depends on the temperature and the frequency of the normal mode,  $\omega_K$ <sup>20</sup>

$$p(q_K) = \frac{1}{x\sqrt{2\pi}} \exp\left(-\frac{q_K^2}{2x^2}\right) \quad (10)$$

where

$$x^2 = \frac{\hbar \left[ 1 + \exp\left(-\frac{\hbar\omega_K}{k_B T}\right) \right]}{2\omega_K \left[ 1 - \exp\left(-\frac{\hbar\omega_K}{k_B T}\right) \right]} \quad (11)$$

### 3. Calculation Details

The evaluation of lattice expansion effect on <sup>17</sup>O and <sup>25</sup>Mg chemical shifts will be referred to as a “static calculation” because the only effect taken into account is the thermal expansion of the MgO structure, measured by Hazen<sup>21</sup> on synthetic single crystals of MgO. Chemical shift calculations taking into account vibrational effects will be referred to as “dynamic calculations”. We considered four different temperatures ranging from room temperature to 1000 °C. The temperatures and corresponding equilibrium volumes are reported in Table 1.

In both cases, the interaction of the electrons with the ion cores are described by norm-conserving pseudopotentials in the Kleinmann–Bylander form<sup>22</sup> generated following a scheme

proposed by Troullier and Martins.<sup>23</sup> Chemical shift calculations are performed<sup>9,24,25</sup> using the PARATEC code<sup>26</sup> and the GGA approximation. We use the Perdew–Burkes–Ernzerhof (PBE) generalized gradient approximation,<sup>27</sup> which gives very similar results to those obtained using the PW91 approximation<sup>28</sup> and corrects some of the numerical instabilities. Pseudopotentials were constructed with  $s$  nonlocality for O and  $s$  and  $p$  nonlocality for Mg. The cores of Mg and O are  $1s^2$ . The core radii of Mg are 1.65 au for the  $2s$ -orbital, 1.09 au for the  $2p$ -orbital, and 1.29 au for the  $3d$  orbital while core radii of oxygen are 1.45 for both  $2s$ - and  $2p$ -orbitals. The wave functions were expanded in plane waves with an energy cutoff of 100 Ry. Convergence was tested at 140 Ry as well. The Brillouin zone sampling included 1  $k$ -point with a  $k$ -grid shift of  $0.25 \times 0.25 \times 0.25$ . The supercell consists of 64 atoms (32 Mg and 32 O).

For each temperature, we calculated the dynamic matrix for the volume indicated in Table 1. The dynamic matrix has been numerically constructed from the force values calculated for an atomic displacement of 0.005 Å for each atom in the supercell. The displacement represents approximately 0.25% of the MgO bond length at room temperature. Forces were calculated using the LDA approximation, which has been shown to give an accurate phonon frequency for MgO.<sup>29</sup> The core–valence electron interaction is described using pseudopotentials generated with the same parameters as for the chemical shift calculations. For the force calculations, the wave functions were expanded in plane waves with an energy cutoff of 140 Ry.

For each temperature  $T$ ,  $N_c$  configurations (Table 1) were generated populating the normal modes  $q$  with the Gaussian probability law given by eq 10. At a temperature  $T$ , we evaluate the integral in eq 7 by averaging the chemical shifts over the 32 oxygen or magnesium atoms in the supercell and over all configurations. We also estimate, for each temperature, the fluctuations of the atoms around their equilibrium positions by computing their average mean-square displacement. The square displacement of atom  $i$ ,  $\langle u_i^2 \rangle_{\text{th}}$ , computed with the distribution of eq 10, is equal to

$$\langle u_i^2 \rangle_{\text{th}} = \frac{\hbar}{2m_i} \sum_{K=1}^{3N-3} \sum_{\alpha} \frac{||\epsilon_{i,\alpha}||^2}{\omega_K} + \frac{\hbar}{m_i} \sum_{K=1}^{3N-3} \sum_{\alpha} \frac{||\epsilon_{i,\alpha}||^2 e^{-\hbar\omega_K/k_B T}}{(1 - e^{-\hbar\omega_K/k_B T})\omega_K} \quad (12)$$

$K$  is an index running through all normal modes (except the three translation modes) of frequency  $\omega_K$  and polarization vector in the direction  $\alpha$ ,  $\epsilon_{i,\alpha}$ ,  $\alpha$  referring to  $x$ ,  $y$ , or  $z$ . The values of  $\langle u_i^2 \rangle_{\text{th}}$  for oxygen and magnesium atoms are reported in Table 1 and compared to the  $\langle u_i^2 \rangle_{\text{conf}}$  for oxygen and magnesium atoms calculated from the configurations.

### 4. Results and Discussion

Experimental results from Fiske and co-workers<sup>4</sup> and the results obtained in this work for both static and dynamic calculations are presented in Figure 1 and Figure 2 for <sup>25</sup>Mg and <sup>17</sup>O, respectively. For reasons of clarity, we have plotted the variation as a function of temperature of the difference between the chemical shift at temperature  $T$  and the chemical shift at room temperature.

Error bars for the dynamic calculation have been evaluated from the statistics arising from the number of configurations  $N_c$ , and the experimental error bar on the chemical shift measurement is the experimental uncertainty of Fiske and co-

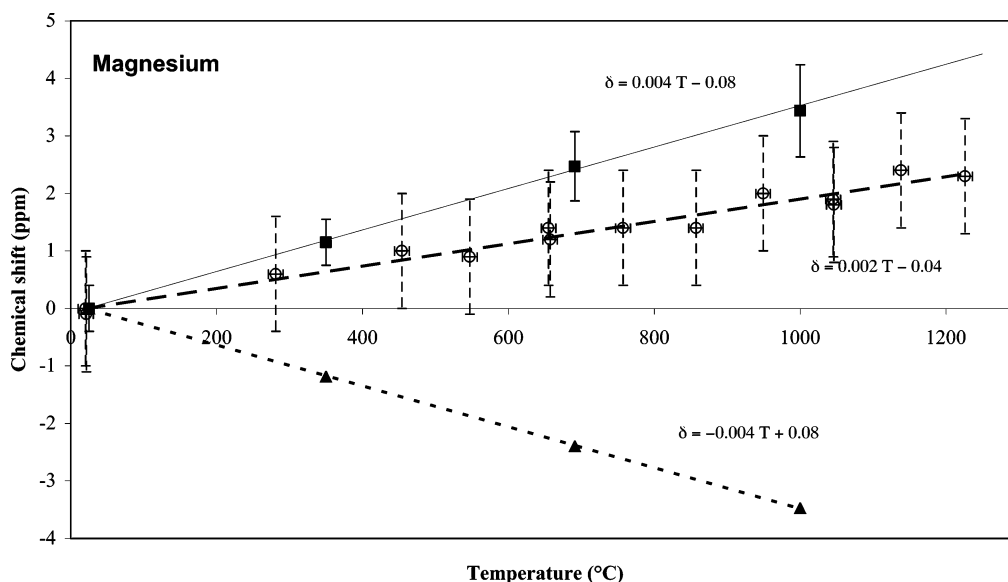


**Figure 1.** Dependence with temperature of the difference between  $^{25}\text{Mg}$  chemical shift at temperature  $T$  and  $^{25}\text{Mg}$  chemical shift at 25 °C (in ppm): experimental data from ref 4 (open circles); static calculation (full triangles); dynamic calculation (full squares). Error bars for each point of the dynamic calculation are given by  $\pm 1.9799\sigma$  where  $\sigma$  is the standard deviation obtained for the  $32N_c$  Mg atoms at each temperature. Error bars on the slope of the best fit lines are  $\pm 0.002$  for the dynamic calculations and  $\pm 0.004$  for experiment.

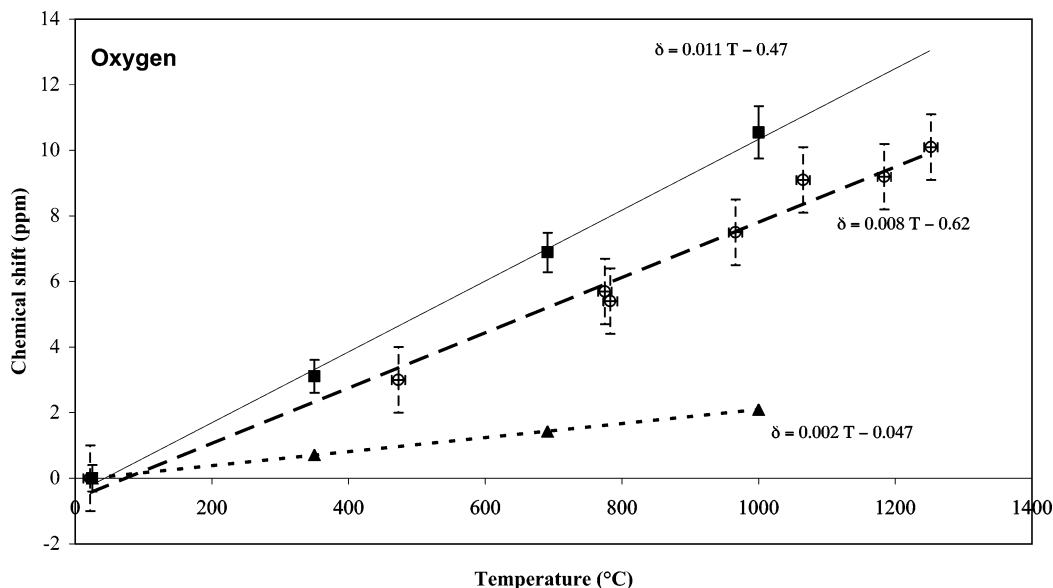


**Figure 2.** Dependence with temperature of the difference between  $^{17}\text{O}$  chemical shift at temperature  $T$  and  $^{17}\text{O}$  chemical shift at 25 °C (in ppm): experimental data from ref 4 (open circles); static calculation (full triangles); dynamic calculation (full squares). Error bars for each point of the dynamic calculation are given by  $\pm 1.9799\sigma$  where  $\sigma$  is the standard deviation obtained for the  $32N_c$  O atoms at each temperature. Error bars on the slope of the best regression lines are  $\pm 0.002$  for the dynamic calculations and  $\pm 0.003$  for experiment.

workers. Because the error bar for the static calculation is due to systematic DFT errors, it is identical for all calculations and is thus not mentioned. Best fit lines have been evaluated using least-squares refinements and assuming that the error in temperature measurement was negligible as compared to the error made on chemical shift. Best fit line equations and error values are given in the graph captions (Figures 1 and 2).

The static calculation, i.e., the variation of the equilibrium Mg–O distance as a function of temperature, cannot alone explain the observed variation of chemical shift as suggested in the work of Fiske and co-workers.<sup>4</sup> Notice, however, that Fiske and co-workers' correct conclusion was based on an incorrect assumption that the Mg–O bond expansion due to temperature could be mimicked by cation substitution. Indeed, it has been shown in a recent publication<sup>7</sup> that the dependence of oxygen shift on the type of alkaline-earth metal is due to the

interaction between the empty d-orbitals of the alkaline-earth cation and the 2p-orbitals of the oxygen atom and not to the metal–oxygen distance. This is also confirmed by the results of the present work. From substitution consideration (see Introduction),  $^{17}\text{O}$  chemical shift deshielding is estimated to be around 20 ppm, while static calculation provided in this work leads to a deshielding of roughly 2 ppm.

In contrast to the static calculations, dynamic calculations reproduce well the experimental trends for both NMR nuclei. Note that the present approach takes into account the fluctuations due to both the thermal excitation and the zero point motion. The agreement between experiment and calculation is very good at low temperature, but at higher temperature, calculations overestimate the chemical shifts as compared to experiment. This discrepancy is not due to a too small of a number of configurations because the average values of the mean-square



**TABLE 2: Absolute Shieldings at 25 °C (in ppm) for Static Calculations with an Energy Cutoff of 140 and 100 Ry, for Dynamic Calculations with an Energy Cutoff of 100 Ry, and for the Experimental Results of Fiske and Co-Workers<sup>4</sup>**

	static (140 Ry)	static (100 Ry)	dynamic	EXP <sub>1</sub> <sup>a</sup>	EXP <sub>2</sub> <sup>b</sup>
$\sigma_{\text{abs}}^{\text{O}}$	199.2	197.5	194.8	240.5	240.9
$\sigma_{\text{abs}}^{\text{Mg}}$	527.8	533.6	531.6		

<sup>a</sup> Using the  $^{17}\text{O}$  absolute scale of Wasylishen et al. (ref 33). <sup>b</sup> Using the  $^{17}\text{O}$  absolute scale of Vaara et al. (ref 10).

displacements of both magnesium and oxygen atoms ( $\langle u_{\text{Mg}}^2 \rangle_{\text{conf}}$  (respectively  $\langle u_{\text{O}}^2 \rangle_{\text{conf}}$ ) in Table 1) are close to the theoretical values ( $\langle u_{\text{Mg}}^2 \rangle_{\text{th}}$  (respectively  $\langle u_{\text{O}}^2 \rangle_{\text{th}}$ ) in Table 1). This discrepancy, however, could be related to the combined effect of failure of the QHA and to the influence of the presence of defects in the MgO bulk structure.

A theoretical study has shown that the QHA is valid for MgO at ambient pressure up to a temperature of 1000 K,<sup>18</sup> by considering the behavior of thermal expansion with temperature. Calculations are shown to overestimate the experimental thermal expansion by 7%. Extrapolated to our study, this result means that chemical shifts at a temperature greater than 1000 K will be overestimated as compared to experiment. Various hypotheses have been proposed to explain this failure of the QHA.<sup>30–32</sup>

It is also possible that the population and behavior of paramagnetic defects affect the chemical shift behavior with temperature. From the experimental point of view, Fiske and co-workers did compare the changes in temperature of the NMR spectra of a single crystal with the ones of a powder.<sup>4</sup> No difference in the peak positions of the two samples were detected up to a temperature of 900 °C. Above that temperature, the powder sample NMR spectra have not been measured. Below 900 °C, we can therefore conclude that the defect population has no detectable influence on the peak positions, suggesting that our calculations based on a perfect MgO structure are correct. We also considered the possibility that a time-averaged, nonzero electric field gradient could lead to a “second-order quadrupolar shift” to low-frequency, thus reducing the magnitude of the paramagnetic shift. However, given the symmetry of the MgO structure, this should not occur. At high temperature, Wang and Reeber suggest that abnormal expansion arises from the dynamical ordering of thermal defects.<sup>31,32</sup> This introduces new defect vibrational modes that respond dynamically to increasing thermal stresses. The critical temperature to observe such an effect is 730 °C.<sup>31</sup> This could participate in the trend that we observe at temperatures higher than 1000 °C.

Theoretical absolute shieldings of  $^{25}\text{Mg}$  and  $^{17}\text{O}$  for various calculations have been reported in Table 2 together with experimental absolute shieldings derived using Wasylishen et al. and Vaara et al. absolute chemical shielding scales.<sup>10,33</sup> To our knowledge, there is no absolute scale established for  $^{25}\text{Mg}$ . The differences between absolute chemical shieldings calculated in the static model at 100 and 140 Ry are due to the fact that at 100 Ry our calculations are not perfectly converged. This is, however, not fundamental to this study because we are mainly interested in the relative effect of temperature on chemical shifts.

There is a large discrepancy between theoretical and experimental absolute shieldings of  $^{17}\text{O}$ , although the variation with temperature is correctly reproduced. This disagreement has already been noted in a previous work<sup>34</sup> and is not yet explained. However, the disagreement observed in both studies is of the same order of magnitude. In Profeta and co-workers’ work, the calculated absolute shieldings on  $\text{SiO}_2$  polymorphs are lower than the experimental ones by around 50 ppm<sup>7</sup> while in this work the calculated absolute shielding is lower than the

experimental one by 65 ppm. This discrepancy cannot be ascribed to a failure of the GIPAW approach, which corrects for the obvious deficiency of pseudopotentials in the prediction of core-dependent properties.<sup>9</sup> Indeed, the absolute shieldings obtained in molecules or solids with GIPAW perfectly reproduce those obtained with the all-electron gauge-including atomic orbitals (GIAO) or individual gauges for atoms in molecules (IGAIM) approaches.<sup>9,34</sup>

Vaara and co-workers have recently refined the absolute scale of  $^{17}\text{O}$  chemical shielding by including rovibrational effects.<sup>10</sup> The use of this refined scale reduced the disagreement between our calculated (194.8334 ppm) and our measured (240.9 ppm) chemical shielding of  $^{17}\text{O}$  in MgO at room temperature from 65 to 45 ppm.

## 5. Conclusion

In this paper, we have presented a new approach for the calculation of rovibrational effects in solids. We consider the fluctuations of the atoms around their equilibrium position using a harmonic Hamiltonian. We applied our approach to the description of temperature dependence of the  $^{17}\text{O}$  and  $^{25}\text{Mg}$  chemical shift in MgO.

Through the use of first-principles calculations, we have shown that the chemical shift variation with temperature cannot be explained by thermal expansion alone. Vibrational corrections due to the fluctuation of atoms around their equilibrium position are crucial to reproduce the experimental results. At 800 °C, the correction is as large as 6.5 ppm for  $^{17}\text{O}$  and 5.5 ppm for  $^{25}\text{Mg}$ . We have shown that these fluctuations can be computed using the quasi-harmonic approximation up to a temperature of 1000 °C.

At temperatures greater than the MgO Debye temperature, the failure of the quasi-harmonic approximation combined with an eventual dynamic ordering of thermal defects imply an overestimation of calculated chemical shifts as compared to experimental ones. At 1000 °C, the magnesium chemical shift is overestimated by 1.5 ppm while the oxygen one is overestimated by 2.5 ppm.

These results are of crucial importance to the correct interpretation of high-temperature data and eventual structural changes. While large changes in chemical shifts with temperature are likely to be due to structural changes, thermal effects will significantly bias chemical shift values at high temperature.

These results, obtained in the case of  $^{17}\text{O}$  and  $^{25}\text{Mg}$  in periclase, should be cautiously extrapolated to other nuclei as thermal effects will affect differently various nuclei as has been observed experimentally.<sup>35</sup>

**Acknowledgment.** We are grateful to Cécile Malgrange, Christian Brouder, Etienne Balan, and Delphine Cabaret for their comments and suggestions, Mikael Profeta for his help with the PARATEC program, and Professor Valentine Genon-Catalot for advice on statistical errors. Special thanks go to Delphine Cabaret for her comments on this manuscript. Calculations were performed at the IDRIS supercomputer center of the CNRS. This research was supported under the Alliance joint research program (PN99.081). C.J.P. is supported by an EPSRC Advanced Research Fellowship.

## References and Notes

- (1) Stebbins, J. F. *Chem. Rev.* **1991**, *91*, 1353.
- (2) Freeman, R.; Murray, G. R.; Richards, R. E. *Proc. R. Soc. London, Ser. A* **1957**, *242*, 455.
- (3) Hafner, S.; Nachtreib, N. H. *J. Chem. Phys.* **1964**, *40*, 2891.

- (4) Fiske, P. S.; Stebbins, J. F.; Farnan, I. *Phys. Chem. Miner.* **1994**, 20, 587.
- (5) Xue, X.; Stebbins, J. F.; Kanzaki, M. *EOS, Trans. Am. Geophys. Union* **1992**, 72, 572.
- (6) Engelhardt, G.; Michel, D. *High-Resolution Solid-State NMR of Silicates and Zeolites*; John Wiley and Sons: New York, 1987.
- (7) Profeta, M.; Benoit, M.; Mauri, F.; Pickard, C. J. *J. Am. Chem. Soc.* **2004**, 126, 12628.
- (8) Tossell, J. A. *Phys. Chem. Miner.* **1998**, 25, 453.
- (9) Pickard, C. J.; Mauri, F. *Phys. Rev. B* **2001**, 63, 245101.
- (10) Vaara, J.; Lounila, J.; Ruud, K.; Helgaker, T. *J. Chem. Phys.* **1998**, 109, 8388.
- (11) Landau, D. P.; Binder, K. *A Guide to Monte Carlo Simulations in Statistical Physics*; Cambridge University Press: New York, 2000.
- (12) Feynman, R. P. *Statistical Mechanics*; Perseus Books: New York, 1998.
- (13) Anderson, O. L.; Isaak, D. L.; Oda, H. *J. Geophys. Res.* **1991**, 96, 18037.
- (14) Inbar, I.; Cohen, R. E. *Geophys. Res. Lett.* **1995**, 22, 1533.
- (15) Chopelas, A. *Phys. Chem. Miner.* **1990**, 17, 142.
- (16) Gavartin, J. L. *J. Phys.: Condens. Matter* **2001**, 13, 10873.
- (17) Isaak, D. G.; Anderson, O. L.; Goto, T. *Phys. Chem. Miner.* **1989**, 16, 704.
- (18) Karki, B. B.; Wentzcovitch, R. M.; de Gironcoli, S.; Baroni, S. *Science* **1999**, 286, 1705.
- (19) Ashcroft, N. W.; Mermin, N. D. *Solid-State Physics*; Saunders College Publishing: Fort Worth, TX, 1976.
- (20) Kleinert, H. *Path Integrals in Quantum Mechanics, Statistics and Polymer Physics*; World Scientific: River Edge, NJ, 1995.
- (21) Hazen, R. *Am. Mineral.* **1976**, 61, 266.
- (22) Kleinman, L.; Bylander, D. M. *Phys. Rev. Lett.* **1982**, 48, 1425.
- (23) Troullier, N.; Martins, J.-L. *Phys. Rev. B* **1991**, 43, 1993.
- (24) Mauri, F.; Louie, S. G. *Phys. Rev. Lett.* **1996**, 76, 4246.
- (25) Mauri, F.; Pfrommer, B. G.; Louie, S. G. *Phys. Rev. Lett.* **1996**, 77, 5300.
- (26) Calculations were performed with PARATEC (parallel total energy code) by B. Pfrommer, D. Raczkowski, A. Canning, S. G. Louie (with contributions from F. Mauri, M. Cote, Y. Yoon, Ch. Pickard, and P. Haynes), Lawrence Berkeley National Laboratory. For more information, see <http://www.nersc.gov/projects/paratec>.
- (27) Perdew, J. P.; Burke, K.; Ernzerhof, M. *Phys. Rev. Lett.* **1996**, 77, 3865.
- (28) Perdew, J. P.; Wang, Y. *Phys. Rev. B* **1992**, 45, 13244.
- (29) Schütt, O.; Pavone, P.; Windl, W.; Karch, K.; Strauch, D. *Phys. Rev. B* **1994**, 50, 3746.
- (30) Karki, B. B.; Wentzcovitch, R. M.; de Gironcoli, S.; Baroni, S. *Phys. Rev. B* **2000**, 61, 8793.
- (31) Reeber, R. R.; Goessel, K.; Wang, K. *Eur. J. Mineral.* **1995**, 7, 1039.
- (32) Wang, K.; Reeber, R. R. *Phys. Status Solidi A* **1994**, 146, 621.
- (33) Wasylishen, R. E.; Bryce, D. L. *J. Chem. Phys.* **2002**, 117, 10061.
- (34) Profeta, M.; Mauri, F.; Pickard, C. J. *J. Am. Chem. Soc.* **2003**, 125, 541.
- (35) Fiske, P. S.; Stebbins, J. F. *Am. Mineral.* **1994**, 79, 848.